Sakamoto, Y. K., and Oshimura M. 2003, A new imprinted cluster on the human chromosome 7q21-q31, identified by human-mouse monochromosomal hybrids, *Genomics*, **81**, 556–559.
17. Yoshioka, H., Shirayoshi, Y., and Oshimura, 2001, M. A novel in vitro system for analyzing parental allele-specific histone acetylation in genomic imprinting, *J. Hum. Genet.*, **46**, 626–632.
18. Inoue, J., Mitsuya, K., Maegawa, S. et al. 2001, Construction of 700 human/mouse A9 monochromosomal hybrids and analysis of imprinted genes on human chromosome 6, *J. Hum. Genet.*, **46**, 137–145.
19. Szeto, I. Y., Li, L. L., and Surani, M. A. 2000, *Ocat*, a paternally expressed gene closely linked and transcribed in the opposite direction to *Peg3*, *Genomics*, **67**, 221–227.
20. Adachi, N. and Lieber, M. R. 2002, Bidirectional gene organization: a common architectural feature of the human genome, *Cell*, **109**, 807–809.
21. Xu, C. F., Brown, M. A., Nicolai, H., Chambers, J. A., Griffiths, B. L., and Solomon, E. 1997, Isolation and characterisation of the *NBR2* gene which lies head to head with the human *BRCA1* gene, *Hum. Mol. Genet.*, **6**, 1057–1062.
22. Herman, J. G., Latif, F., Weng, Y. et al. 1994, Silencing of the VHL tumor-suppressor gene by DNA methylation in renal carcinoma, *Proc. Natl. Acad. Sci. USA*, *91*, 9700–9704.
23. Merlo, A., Herman, J. G., Mao, L. et al. 1995, 5′ CpG island methylation is associated with transcriptional silencing of the tumour suppressor *p16/CDKN2/MTS1* in human cancers, *Nat. Med.*, **1**, 686–692.
24. Herman, J. G., Jen, J., Merlo, A., and Baylin, S. B. 1996, Hypermethylation-associated inactivation indicates a tumor suppressor role for $p15^{INK4B}$, *Cancer Res.*, **56**, 722–727.
25. Dobrovic, A. and Simpfendorfer, D. 1997, Methylation of the *BRCA1* gene in sporadic breast cancer, *Cancer Res.*, **57**, 3347–3350.
26. Stirzaker, C., Millar, D. S., Paul, C. L. et al. 1997, Extensive DNA methylation spanning the *Rb* promoter in retinoblastoma tumors, *Cancer Res.*, **57**, 2229–2237.
27. Graff, J. R., Herman, J. G., Lapidus, R. G. et al. 1995, *E-cadherin* expression is silenced by DNA hypermethylation in human breast and prostate carcinomas, *Cancer Res.*, **55**, 5195–5199.
28. Kim, J., Kollhoff, A., Bergmann, A., and Stubbs, L. 2003, Methylation-sensitive binding of transcription factor YY1 to an insulator sequence within the paternally expressed imprinted gene, *Peg3*, *Hum. Mol. Genet.*, **12**, 233–245.

Human Molecular Genetics, 2004, Vol. 13, No. 23 *2959–2969*
doi:10.1093/hmg/ddh313
Advance Access published on September 30, 2004

Allelic expression imbalance of the human *CYP3A4* gene and individual phenotypic status

Takeshi Hirota[1], Ichiro Ieiri[2,*], Hiroshi Takane[2], Shinji Maegawa[3], Masakiyo Hosokawa[5], Kaoru Kobayashi[5], Kan Chiba[5], Eiji Nanba[3], Mitsuo Oshimura[4], Tetsuo Sato[5], Shun Higuchi[1] and Kenji Otsubo[2]

[1]Clinical Pharmacokinetics, Division of Clinical Pharmacy, Graduate School of Pharmaceutical Sciences, Kyushu University, Fukuoka 8128582, Japan, [2]Department of Hospital Pharmacy, Faculty of Medicine, [3]Division of Functional Genomics, Research Center for Bioscience and Technology and [4]Department of Biomedical Science, Institute of Regenerative Medicine and Biofunction, Graduate School of Medical Science, Tottori University, Yonago 6838504, Japan and [5]Laboratory of Biochemical Pharmacology and Toxicology, Graduate School of Pharmaceutical Sciences, Chiba University, Chiba 2740816, Japan

Received August 6, 2004; Revised and Accepted September 20, 2004

The human cytochrome P450 3A4 (CYP3A4) plays a dominant role in the metabolism of numerous clinically useful drugs. Alterations in the activity or expression of this enzyme may account for a major part of the variation in drug responsiveness and toxicity. However, it is generally accepted that most of the known single nucleotide polymorphisms in the coding and 5′-flanking regions are not the main determinants for the large inter-individual variability of CYP3A4 expression and activity. We show that the allelic variation is critically involved in determining the individual total hepatic CYP3A4 mRNA level and metabolic capability. There exists a definite correlation between the total CYP3A4 mRNA level and allelic expression ratio, the relative transcript level ratio derived from the two alleles. Individuals with a low expression ratio, exhibiting a large difference of transcript level between the two alleles, revealed extremely low levels of total hepatic CYP3A4 mRNA, and thus low metabolic capability as assessed by testosterone 6β-hydroxylation. These results present a new insight into the individualized CYP3A4-dependent pharmacotherapy and the importance of expression imbalance to human phenotypic diversity.

INTRODUCTION

Among the human cytochrome P450 (CYP) proteins, the members of the CYP3A subfamily occupy an important position owing to their abundance in liver and gut and to their collective large substrate spectrum (1). CYP3A proteins account for up to 50% of total CYP activity in the liver, and they metabolize up to 60% of all drugs currently in use (2,3). Cytochrome P450 3A4 (CYP3A4) is the major form of CYP in human liver; accounting for 30% of total CYP protein content (4). A wide inter-individual variation exists in CYP3A4 activity as assessed by direct analysis of liver microsomes (4) and through the use of *in vivo* probe drugs (5). The basis of this variation is not yet understood but may be due to genetic factors. A clinical study with CYP3A4 substrates suggested that ~60–90% of the inter-individual variability in hepatic CYP3A4 activity is genetically determined (6). The coding and 5′-flanking regions of the *CYP3A4* gene have been isolated and sequenced, and some single nucleotide polymorphisms (SNPs) have been identified; however, their allelic frequencies and/or the available functional experiments indicate a limited role for these variants in the inter-individual variability of CYP3A4 expression and activity (7–12).

In addition to SNPs, various gene expression mechanisms have recently been reported to determine phenotypic variability; these patterns include genomic imprinting (13,14), X-chromosome inactivation (15) and other mechanisms (16,17). Among them, genomic imprinting is an epigenetic phenomenon where parental alleles are genetically marked, leading to the differential expression of paternal and maternal alleles in somatic cells (13,14). Imprinting genes are often clustered in chromosomal domains and are thought to

*To whom correspondence should be addressed at: Department of Hospital Pharmacy, Faculty of Medicine, Tottori University, Nishi-machi 36-1, Yonago 6838504, Japan. Tel: +81 859348385; Fax: +81 859348087; Email: ieiri@grape.med.tottori-u.ac.jp

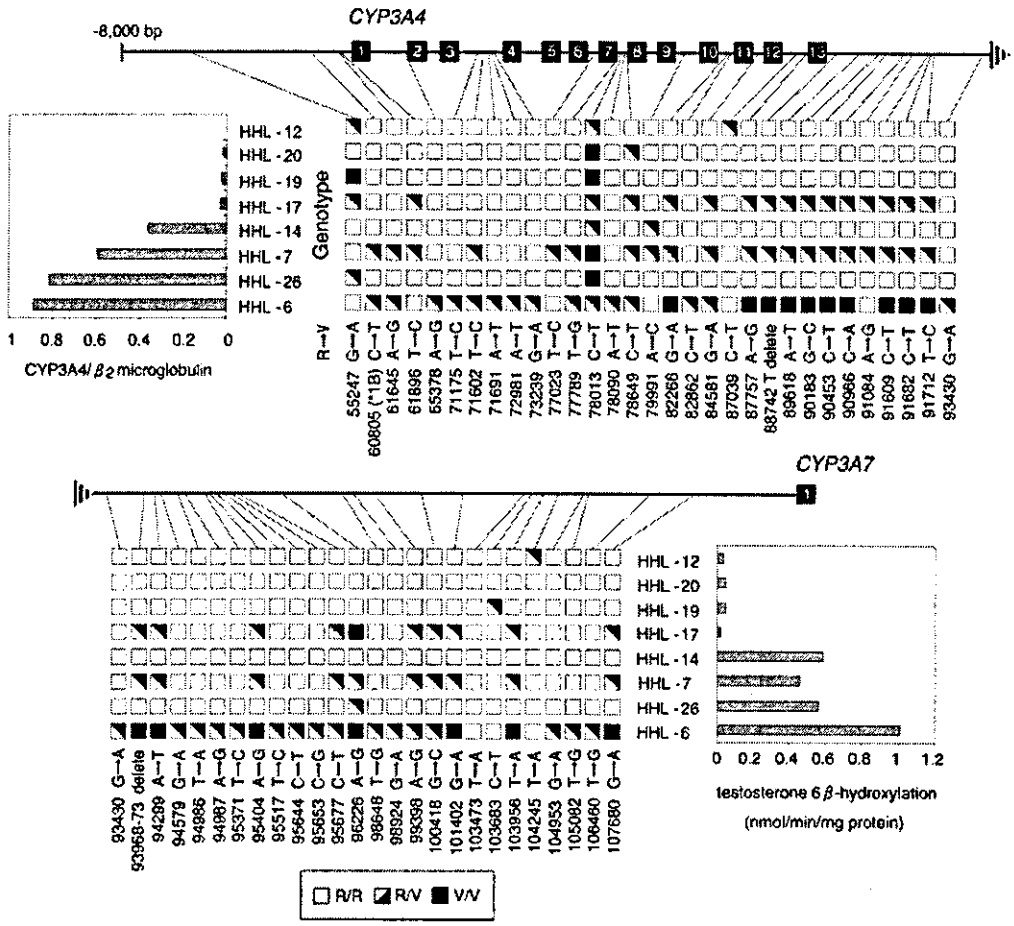

Figure 1. Relationship between CYP3A4 phenotypes and *CYP3A4* genotype in Caucasian livers. Open, partially filled and closed squares correspond to liver homozygous for the reference sequence (R), and heterozygous and homozygous for the variant sequence (V).

be coordinately regulated by imprinting control centers (13,18). Interestingly, three members of the CYP3A subfamily, *CYP3A4*, *CYP3A5* and *CYP3A7*, are localized in tandem on the long arm of chromosome 7 at q21–q22.1 (19,20), where several imprinted genes are clustered (21). In addition, differences in expression levels between the two alleles of the same gene (i.e. preferential expression of one of the two alleles), which were not consistent with parental imprinting, have been reported in various genes such as *PKD2*, *p73* and *Calpain-10* (16,22). Some investigators indicated that such allelic variation in gene expression was common in the human genome (17,22). The individual allelic expression status may result in a change in the expression level of the gene (23,24), leading to phenotypic variability in the pharmacokinetic and pharmacodynamic outcomes of drug therapy. On screening the entire *CYP3A4* gene, we found two common non-functional and racially independent intronic SNPs, C78013T (C → T at nt 78013) and C78649T (C → T at nt 78649), and used them as markers in subsequent gene expression analyses. Using these SNPs, we elucidated that the allelic variation is critically involved in the hepatic CYP3A4 mRNA expression. Individuals with a low expression ratio, exhibiting a large difference of transcriptional level between the two alleles, revealed extremely low hepatic CYP3A4 levels and thereby reduced metabolic activity. These findings explain the substantial inter-individual differences in CYP3A4 expression and activity.

RESULTS

Screening of the marker SNPs for assessment of allelic variation

To screen the marker SNPs for assessment of allelic variation and to evaluate the presence of functional *CYP3A4* gene variants, we amplified and sequenced the whole *CYP3A4* gene, *CYP3A4* 5′-flanking region and 3′-untranslated region (UTR), spanning ~60 kb, using genomic DNAs extracted from eight Caucasian liver samples with high (HHL-6, -7, -14 and -26) or low (HHL-12, -17, -19 and -20) levels of total CYP3A4 mRNA (Fig. 1). The former and latter samples also indicated high and low testosterone 6β-hydroxylation

activity, respectively. In the present study, testosterone 6β-hydroxylation capability was used as an index for individual CYP3A4 activity. We identified 4, 35 and 17 polymorphisms in the 5′-flanking region, 3′-UTR and intronic region, respectively, but did not find any coding SNPs. Although three samples, HHL-6, HHL-7 and HHL-17, had many SNPs in the regions analyzed, the other samples had only 2–4 SNPs. Among them, frequencies of the C78013T (8/8) and C78649T (4/8) polymorphisms were relatively high. Thus, we used these two intronic SNPs as markers in the subsequent gene expression study.

We next examined the association of the allelic pattern with total hepatic CYP3A4 mRNA levels. Although the CYP3A4 level was comparable between HHL-6 and HHL-26, the SNP patterns were clearly different. In contrast, there were remarkable differences in the CYP3A4 levels between HHL-7 and HHL-17 even though the SNP pattern was similar. In addition to the total mRNA levels, a similar trend was observed in the testosterone 6β-hydroxylation activity. As has previously been demonstrated (7–12), these results suggest that SNPs in these regions are not involved in the large variability in the *CYP3A4* gene expression and metabolic activity.

Correlation between total hepatic CYP3A4 mRNA levels and CYP3A4 hnRNA levels

We next examined whether tissue levels of heterogeneous nuclear RNA (hnRNA), the unprocessed precursor of the mature, functional mRNA, can be used as a surrogate for gene transcription. CYP3A4 hnRNA and total mRNA levels were determined in a total of 18 hepatic samples. Quantification of total CYP3A4 mRNA and hnRNA was performed by the real-time PCR method. As shown in Figure 2, CYP3A4 mRNA showed significant regression ($r = 0.775$; $P < 0.001$). These results validated the use of CYP3A4 hnRNA as an estimate of CYP3A4 gene activity in human liver samples.

Allelic variations in human liver samples

Prior to evaluating the functional significance of allelic variation in total hepatic CYP3A4 mRNA levels and metabolic activity, we estimated allelic expression ratios, defined as a measure of the expression of the less-abundant allele divided by that of the more-abundant allele, in order to confirm inter-individual variation in the allelic expression of *CYP3A4*. As described in more detail in the Materials and Methods, allelic variation was determined on the basis of difference in band intensities between the two alleles using a fluorescence image analyzer. When an individual is heterozygous for a marker SNP, it is possible to detect the relative abundance of allelic transcripts. Generally, both copies of human autosomal genes are assumed to be co-dominantly expressed in equal proportions. The detection of allelic variation is based on a quantitative analysis of RNA transcripts in order to detect deviations from the expected equimolar ratio between two alleles in a heterozygous sample. After the screening of genomic DNA from all 40 Caucasian liver samples, it was possible to identify 18 individuals who were heterozygous for either the *Mnl*I (C78013T) or *Aci*I (C78649T) site.

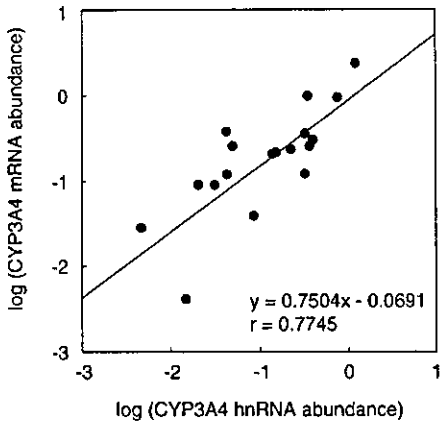

Figure 2. Relationship of total CYP3A4 mRNA and hnRNA levels in human liver samples. A simple linear regression analysis was performed.

The difference in expression between the two alleles varied among samples (Fig. 3), and some of the 18 individuals had fractional allelic expression values lower than the 95% confidence interval for the mean (0.70 ± 0.20; 95% confidence interval, 0.60–0.80). Notably, the values in HHL-12 (0.28), HHL-16 (0.45), HHL-20 (0.46) and HHL-36 (0.49) were extremely low, being well outside the intervals, indicating monoallelic expression. Preferentially expressed allele in an individual sample was also shown in Figure 3. Predominantly expressed allele was different among samples, suggesting that both marker SNPs have no significant effects on the expression of the *CYP3A4* gene.

Allelic expression pattern in informative lymphoblasts

To determine whether the two alleles of the human *CYP3A4* gene are differentially expressed according to parental origin, we used reverse transcription–polymerase chain reaction (RT–PCR) of total RNA extracted from Epstein–Barr (EB) virus-transformed lymphoblasts, followed by PCR–RFLP. The parental origin of alleles expressed in children was identified by RFLP analysis. Lymphoblasts were obtained from a panel of 22 healthy Japanese individuals who were members of six distinct families. These samples allowed the precise determination of the parental origin of alleles in the heterozygous children. Of all the cases, two siblings were heterozygous for a polymorphism at either the *Mnl*I site (C78013T in intron 7) or the *Afa*I site (G82266A in intron 10) (Fig. 4A). As the SNPs used here are in intronic regions of *CYP3A4*, the cDNA analyzed represents unspliced, hnRNA (25). Thus, all RT reactions in the present study included a negative control to ensure that genomic DNA did not contaminate the subsequent PCR. We firstly determined the parent's genotypes using genomic DNA samples. At the *Mnl*I site (for C1 in Fig. 4B and C), although the maternal genotype was homozygous for the T78013 allele, the paternal genotype was heterozygous for the C78013 allele. At the *Afa*I site (for C2), the corresponding genotypes were homozygous for the G82266 allele and heterozygous for the A82266 allele, respectively. In the RT–PCR products, in contrast to C1, who showed a

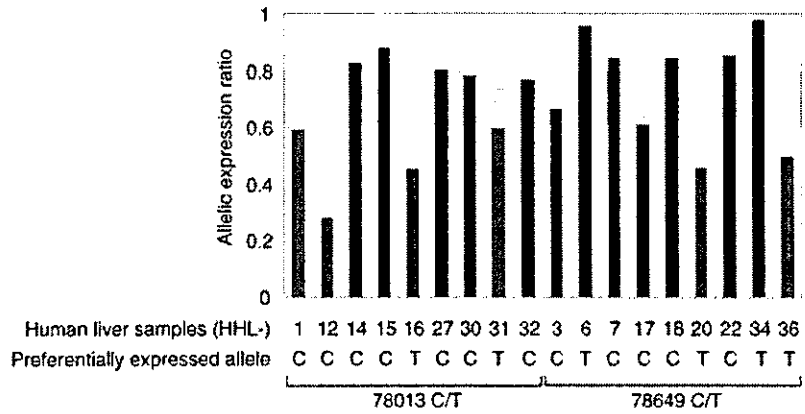

Figure 3. Allelic expression ratio of the *CYP3A4* gene in Caucasian livers. The expression ratio (*y*-axis) was estimated on the basis of the average less-/more-abundant ratios (replicated data-points for each sample) at either the C78013T or the C78649T polymorphism, and corrected using the average genomic ratio. The shaded box represents ~95% confidence interval and the red bars indicate individuals displaying significant variation.

monoallelic maternal (T78013) expression, the sibling C2 showed a biallelic expression, but the paternal allele (A82266) was preferentially expressed.

It is interesting to know whether allelic variation is inherited. In order to address this issue, we further analyzed allelic expression patterns using paternal RT–PCR products, because paternal genotype was heterozygous for both polymorphic sites (at genomic DNA-based genotypes). As shown in Figure 4B, paternal alleles were inherited by the two siblings; the paternal inactive allele (i.e. unexpressed C78013 allele at the *Mnl*I site) and active allele (i.e. expressed A82266 allele at the *Afa*I site) were inherited by siblings C1 and C2, respectively. These results suggest that allelic variation is inherited, at least in B virus-transformed lymphoblasts.

Methylation status in the most proximal 5′-CpG island of the *CYP3A4* gene

We focused on the most proximal 5′-CpG island (covering ~450 bp), which is ~30 kb upstream of the translational start codon, and examined the association of the methylation status with total CYP3A4 mRNA levels using six liver samples; samples HHL-6, -7 and -14 had high and HHL-12, -19 and -20 had low mRNA levels (Fig. 1). The percent methylation of the 31 CpG sites analyzed in the *CYP3A4* CpG island was calculated. Although differentially methylated CpG sites were found, most of the sites analyzed were largely methylated (Fig. 5). No clear association between the methylation status and total mRNA levels was observed.

Allelic variation and CYP3A4 phenotypes

Correlations between the allelic expression ratio and phenotype indexes are shown in Figure 6. The total hepatic CYP3A4 mRNA level correlated strongly with the allelic ratio (Fig. 6A; $r^2 = 0.786$, $P < 0.001$). Of these 18 samples, we could measure CYP3A4 activity using testosterone as an enzyme-specific substrate in 10. As expected, 6β-hydroxylation capability also correlated strongly with the allelic ratio (Fig. 6B; $r^2 = 0.541$, $P < 0.05$). These results indicate that the individuals with a low ratio, who exhibited a large difference in hnRNA expression level between the two alleles, have extremely low total hepatic CYP3A4 mRNA levels, and consequently poor metabolic capability.

Frequency of the two marker SNPs in different racial populations

We determined frequencies of heterozygous carriers for C78013T and C78649T polymorphisms, which were relatively common among the eight liver samples, using genomic DNA from three racial populations (Table 1). We found that the frequency of heterozygous carriers of the C78013T allele in Caucasians was 0.35; in Japanese, 0.39; and in African Americans, 0.56. The corresponding values for the C78649T allele were 0.21, 0.16 and 0.36, respectively. When excluding individuals having two SNPs simultaneously, 50.0% of Caucasians, 41.7% of Japanese and 61.5% of African Americans were heterozygous for either SNP.

DISCUSSION

Variations in gene sequence and expression underlie much of human variability. To decide individual gene expression status, we first sequenced the whole *CYP3A4* gene, *CYP3A4* 5′-flanking region and 3′-UTR using liver tissues from eight Caucasians, and then examined the association of SNP patterns with total CYP3A4 mRNA levels and testosterone 6β-hydroxylation capability. Although the observed nucleotide diversity in the *CYP3A4* promoter was 1 in 7246 bp in Caucasians (26), two recent reports provided evidence for the existence of a specific *cis*-acting element, 8000 bp distal to the transcription start point, which plays an important role in the transcriptional induction of CYP3A4 (27,28). Thus, we analyzed the *CYP3A4* 5′-flanking region, spanning 8 kb. As has been expected, none of the SNPs in these regions was clearly associated with differences in CYP3A4 levels and metabolic capability. These findings raise the possibility

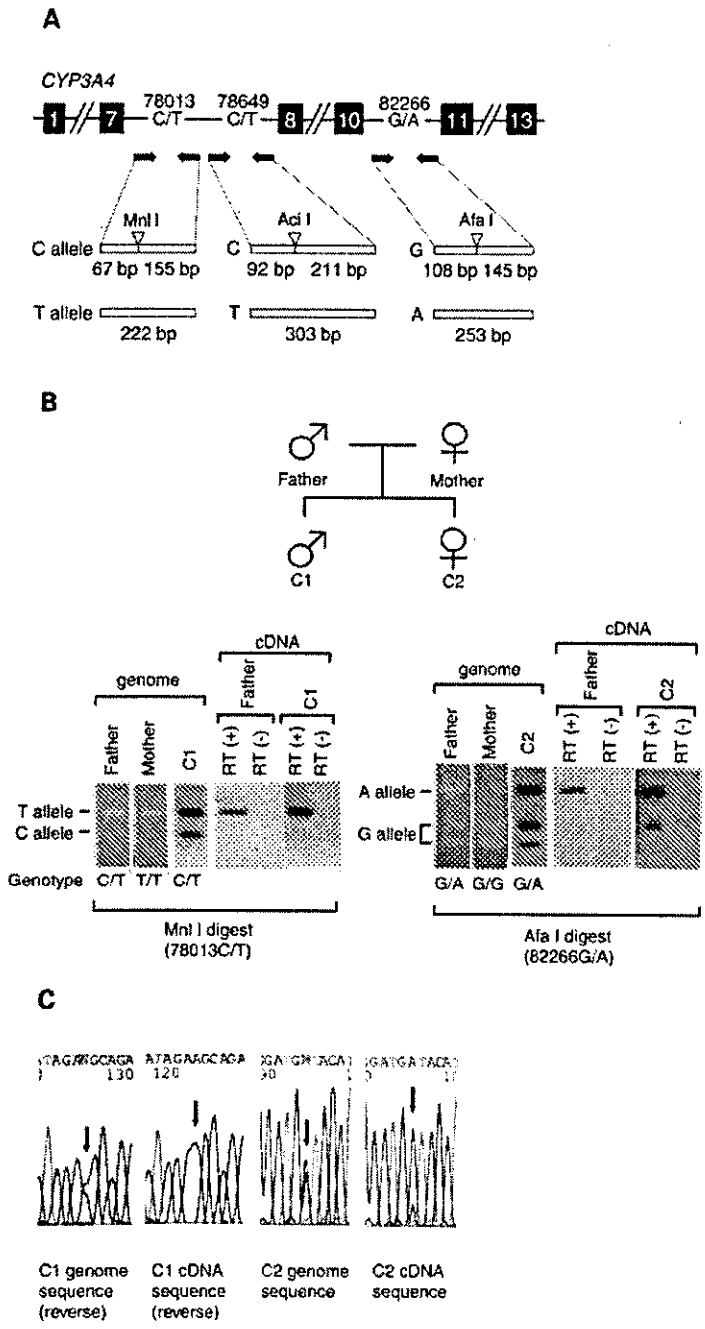

Figure 4. Identification of allelic variation of the *CYP3A4* gene. (**A**) Schematic of the PCR–RFLP for the three polymorphisms. Black squares denote *CYP3A4* exons. Locations of PCR primers are indicated by arrows. Predicted RFLP products of each polymorphism are drawn below the schematic. (**B**) Actual expression patterns in lymphoblasts obtained from two informative siblings. (**C**) Validation of the allelic variation by sequencing.

that other mechanisms such as an epigenetic gene alteration affect CYP3A4 levels more frequently than SNPs (7–12).

In the present study, we used unspliced hnRNA as the template and used intronic SNPs as the marker to assess the allelic variation, because there were no exonic SNPs that can be used to test for allelic variation in mRNA levels. Thus, we secondarily examined whether tissue levels of hnRNA, the unprocessed precursor of the mature, functional mRNA, can be used as a surrogate for gene transcription. To ensure precise determinations for hnRNA and mRNA levels separately,

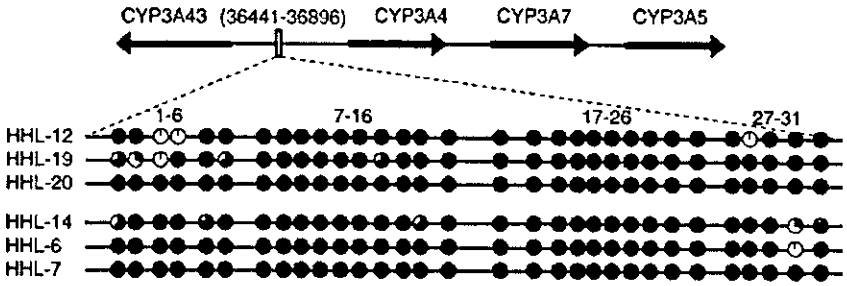

Figure 5. Methylation analysis of the CpG island of the *CYP3A4* gene. Bisulfite PCR products were subcloned and sequenced. The degree of methylation on each CpG dinucleotide was obtained from 20 individual clones. Open and closed areas represent unmethylated and methylated CpG dinucleotides, respectively.

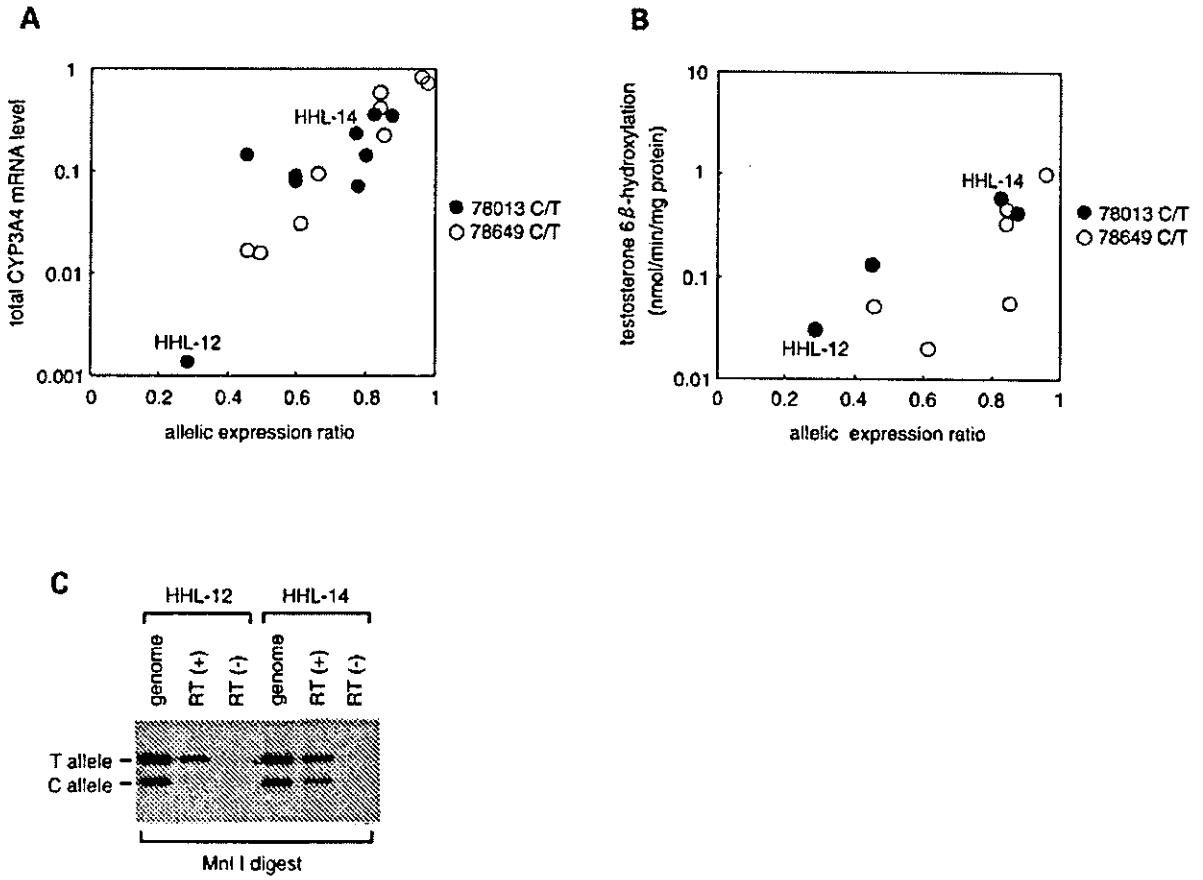

Figure 6. Allelic expression ratio and CYP3A4 phenotypes in Caucasian livers. (A) Relationship between total mRNA level (*y*-axis) and allelic ratio. The ratio was estimated based on the average less-/more-abundant ratios at either the C78013T or the C78649T polymorphism. (B) Relationship between testosterone 6β-hydroxylation capability and allelic ratio. The numbers are identical with the sample numbers in Figures 1 and 3. (C) Actual expression patterns in the livers.

we have designed intron- and exon-specific oligonucleotide primers, respectively. As shown in Figure 2, the two exhibited a significant correlation. These results validated the use of CYP3A4 hnRNA as an estimate of *CYP3A4* gene activity in human liver samples, and suggest that total CYP3A4 mRNA levels are controlled at a point upstream of the precursor by the transcriptional generation of hnRNA (29,30).

Recently, in order to determine allelic variation, an allele-specific quantitative PCR method with allele-specific probes has been developed. Such an analytical method provides the direct expression level of each allele separately by measuring the fluorescent intensity (22,31). In the present study, we had also tried to develop a real-time quantitative PCR method; however, we were unsuccessful owing to a technical limitation,

Table 1. Heterogeneous carriers for *CYP3A4* mutations in different racial populations

Position	Reference allele (R)	Variant allele (V)	Population	Genotype R/R	R/V	V/V	Frequency of heterogeneous carriers
78013	ctgcCtcta	ctgcTtcta	Caucasian	8	34	54	0.35 (0.25–0.45)
			Japanese	6	37	53	0.39 (0.29–0.49)
			African American	9	54	33	0.56 (0.46–0.66)
78649	gtagCggtg	gtagTggtg	Caucasian	74	20	2	0.21 (0.13–0.29)
			Japanese	80	15	1	0.16 (0.09–0.23)
			African American	4	35	56	0.36 (0.26–0.46)

Values in parentheses indicate 95% confidence interval.

low expression levels of CYP3A4 hnRNA, especially in samples indicating monoallelic expression. Thus, we determined allelic variations on the basis of difference of band intensities between the two alleles using a fluorescence image analyzer. With such an analytical method, in addition to DNA contamination, splicing variants are drawbacks for the accurate estimation of allelic variation. In the *CYP3A4* gene, one variant, *CYP3A4*6*, with an insertion of adenine at position 17776, has been reported to create premature mRNA because the variant causes a frame shift and an early stop codon in exon 9 (32). However, the *CYP3A4*6* variant was not observed in our liver samples (data not shown), and this finding was in keeping with previous reports that it has not been observed in Caucasian populations (33,34).

Differential allelic gene expression resulting from genomic imprinting has been a focus of cancer research. Among known imprinted genes, the Wilms' tumor suppressor gene (*WT1*) has been reported to exhibit a unique allele-specific expression profile (35); cultured human fibroblasts and lymphocytes showed a paternal or biallelic expression of *WT1* in some cases, whereas a maternal or biallelic expression was observed in human placental villi and fetal brain tissue (36,37). These results suggest that the allele-specific expression profile (e.g. allele switching) of certain genes depends on the tissue source. Indeed, although somatic allele switching is not a common feature of imprinted genes, this unusual phenomenon is also observed in human *H19* (38) and *IMPT1* (39) genes. However, in the present study, the degree of difference in the expression between the two alleles varied among samples, and large variations were observed in only a minority of samples (Fig. 3). In addition, informative lymphoblast samples indicated opposite-directional expression; both paternal and maternal preferential expressions were observed in the two siblings (Fig. 4). Thus, taking these findings into consideration, it is feasible that, at least in human liver, *CYP3A4* is not an imprinting gene.

Although allelic variation in gene expression is common in the human genome (17,22), its pharmacokinetic and pharmacodynamic significance has not been reported. One study has demonstrated that the allelic variation in *APC* gene expression plays a critical role in colon cancer (16). The present study, however, is the first to demonstrate that variations in CYP3A4 phenotypes are caused by changes in allelic expression levels. The strong correlation between the allelic ratio and phenotypic indexes (e.g. total hepatic mRNA level and testosterone 6β-hydroxylation activity) indicates that individuals having low ratios, who exhibit a large difference in hnRNA expression levels between the two alleles, have extremely low levels of total CYP3A4 mRNA and thereby reduced metabolic activity. Human CYP3A activity reflects the heterogeneous expression of at least two CYP3A family members, CYP3A4 and CYP3A5. Although the role of CYP3A5 in testosterone 6β-hydroxylation *in vivo* has not been defined (40), this heterogeneity is a possible reason for the lower correlation observed between the allelic ratio and hydroxylation activity.

Although not much is known about mechanisms regulating the constitutive basal expression of the *CYP3A4* gene in human tissues, currently available data indicate that numerous transcriptional factors such as hepatocyte nuclear factor-1 (HNF-1), HNF-2, HNF-4 and CCAAT/enhancer-binding protein (C/EBP) regulate the constitutive expression of CYP genes (41). Liver-enriched transcription factors C/EBP and HNF-3γ, which are involved in the regulation of numerous liver-specific genes (42), *trans*-activate and cooperatively regulate hepatic-specific *CYP3A4* gene expression (43,44). Because these liver-enriched *trans*-activating factors play an important roles in the constitutive expression of *CYP3A4*, variations in their expression could ultimately be responsible for the different expression levels of *CYP3A4* found in various human tissues; *CYP3A4* is expressed primarily in liver and intestine and at very low and physiologically insignificant levels in lymphoblasts (45). Although transcriptional elements in lymphoblasts are suggestive of a limited expression (low or absent), allelic variation was clearly observed in lymphoblasts as well as in liver samples (Figs 4 and 6). Thus, these results suggest that it is unlikely that the transcriptional elements described earlier are involved in the allelic imbalance.

Initially in the present study, we could not find any functional SNPs in the *CYP3A4* gene. These results suggest that the post-transcriptional regulation of *CYP3A4* gene expression is likely to be similar for both alleles. As a majority of the differentially expressed genes have a virtually identical sequence in their mRNAs (46), transcriptional initiation by *cis*-acting components is one of the most important controls in regulating the variation in allelic gene expression. The deviation of allelic variation varied among samples (Fig. 3), which also suggests that the variation could result from the allelic heterogeneity of one or more *cis*-acting regulatory polymorphisms (47) or from epigenetic factors such as DNA methylation (48) and the existence of non-coding RNAs (49). In this regard, we examined methylation status in the CpG island,

which is ~30 kb upstream of the translational start codon, using six Caucasian liver samples with high and low levels of total CYP3A4 mRNA by cloning and sequencing bisulfite-treated DNA. However, unfortunately, we did not observe allele-specific differential methylation (Fig. 5).

Recently, Lo *et al.* (22) reported that 326 of 602 genes showed a preferential expression of one allele, and 170 of those showed greater than a 4-fold difference between the two alleles. Interestingly, some of the genes that showed a skewed allelic expression were located next to each other (i.e. clustered), and a subset of these genes is located in known imprinting domains. *ASB4*, *DLX5*, *SGCE* and *PEG10*, which have previously been reported to be imprinted, are located in the imprinting domain at 7q21–q31 (21). The human *CYP3A* genes, *CYP3A43*, *CYP3A4*, *CYP3A7* and *CYP3A5*, consist of a cluster spanning 231 kb within this domain, at 7q21–q22.1 (19,20). In addition, two *CYP3A* pseudogenes are formed in two intergenic regions (*CYP3A4–CYP3A7* and *CYP3A7–CYP3A5*) (50). These unique gene-structural features suggest that the allelic variation in hepatic CYP3A4 expression can be attributed to unknown non-coding RNA(s). The paternally expressed non-coding RNA (*Air* RNA) overlapping one of three imprinted, maternally expressed protein-coding genes (*Igf2r/Slc22a2/Slc22a3*) has been reported to play an important role in repression of all three genes on the paternal expression (49). Nevertheless, we cannot exclude the possibility that the cis-acting regulatory polymorphisms (47) responsible for the change in CYP3A4 expression reside far up- and downstream of the gene of the affected allele. Indeed, Wojnowski and Brockmoller (51) have recently indicated a hepatic transcriptional imbalance of the *CYP3A5* gene in *CYP3A5*1A/*3* heterozygous samples, and the *cis*-acting *1A variant, which increases the expression of the *CYP3A5* gene transcript from the allele carrying the variant, is a possible mechanism for the imbalance.

One report provided evidence that allelic variation can be transmitted by Mendelian inheritance (16). As shown in Fig. 4B, our results indicated that the allelic variation of *CYP3A4* expression was also inherited, as has been observed in the genes *Calpain-10* and *PKD2* (16). Yan *et al.* (16) identified three informative families and found that altered expression of the genes *CAPN10* and *PKD2* was consistently inherited with a single haplotype defined by at least two adjacent microsatellite markers. In contrast to the findings by Yan *et al.* (16), although the allelic variation of *CYP3A4* expression was consistent with Mendelian inheritance, allelic expression ratio appeared to be independent from genotypes. In the present study, we had tried to find the useful haplotypes within the regions we had analyzed; however, we were unsuccessful owing to large inter-individual variability in the SNP pattern (Fig. 1). The mechanism that generates allelic variation between two alleles remains unclear. However, as the expression of *CYP3A4* is unlikely to be regulated by imprinting, these results also suggest the existence of unknown, unidentified *cis*-acting inherited variations influencing gene expression. If *cis*-acting inherited variations in gene expression are common among normal populations, an insight into how this occurs in individuals may help us to understand the large variability in CYP3A4 phenotypes.

MATERIALS AND METHODS

Population samples

We examined allelic frequencies of C78013T and C78649T mutations in genomic DNA samples from unrelated Caucasian, Japanese and African American volunteers (96 subjects each) (Tennessee Blood Services, Memphis, TN, USA). We also obtained samples from the following sources: 22 lymphoblast samples for which the parental origin of the *CYP3A4* alleles was determined (35); 18 livers (selected from 40 Caucasian donors, National Disease Research Interchange, Philadelphia, PA, USA) for which allelic expression variations and total hepatic CYP3A4 mRNA and hnRNA levels were determined, and 10 of the 18 liver samples in which testosterone 6β-hydroxylation capabilities had been analyzed. We sequenced the *CYP3A4* gene, 5′-flanking region and 3′-UTR in eight of the 18 liver samples whose total CYP3A4 mRNA and hnRNA levels had been determined. We also determined methylation status in six of the 18 liver samples. EB virus-transformed lymphoblast cultures were obtained using standard procedures. This study was approved by the Ethical Board of the Faculty of Medicine, Tottori University and informed consent was obtained from all individuals.

Primers and sequencing

We designed 72 primer sets based on a published sequence (GenBank accession no. AF280107.1) to amplify the *CYP3A4* gene, *CYP3A4* 5′-flanking region and 3′-UTR; the amplicons were ~900 bp long (sequence available on request). Primer pairs were used for 30–40 cycles to amplify genomic DNA. The following conditions were used in each cycle: 95°C for 40 s, 52°C for 45 s, and 72°C for 1 min. PCR products were sequenced either directly or after subcloning using BigDye Terminator (Applied Biosystems, Foster City, CA, USA) sequencing. The sequencing primers were those used in the PCR amplifications. The sequence of both strands was analyzed for products from at least two independent PCR amplifications to ensure that the identified mutations were not PCR-induced artifacts.

cDNA synthesis

Total RNA was extracted with an RNAeasy Kit (Qiagen, Hilden, Germany) from EB virus-transformed lymphoblasts and liver samples. Prior to RT, total RNA samples were first treated with RNase-free DNase I, and then digested with *Hae*III and *Mbo*II (Takara, Kyoto, Japan). *Hae* III and *Mbo*II digest the potential DNA template which would lead to the amplification of both alleles and thus mask allelic variation. The RNA samples were then reverse-transcribed into first strand cDNA with 1 μg of total RNA, 4 μl of 5 × first strand buffer, 4 μl of 0.1 mM DTT, 1 μl of 500 μg/ml random primer (Promega, Madison, WI, USA), 4 μl of 10 mM dNTP mixture and 200 U of SuperScript II RNase H⁻ reverse transcriptase (Life Technologies, Rockville, MD, USA). The reaction was incubated at 42°C for 60 min. RT reactions were always carried out in the presence or absence of reverse transcriptase to ensure that genomic DNA did

not contaminate the subsequent PCR. In all experimental procedures, no amplification was detected in the absence of RT, excluding DNA contamination.

Assessment of allelic variation (estimation of allelic expression ratio)

To assess allele-specific expression of *CYP3A4*, an *MnlI* RFLP and an *AciI* RFLP in intron 7 (for liver samples), and an *MnlI* RFLP in intron 7 and an *AfaI* RFLP in intron 10 (for lymphoblast samples) were analyzed. Primer sequences for cDNA amplification were as follows: *MnlI* RFLP, 5′-TATCAG CCCCCTGTCACAAAC-3′ (forward) and 5′-TTCATGCCA CAACATAGTAAA-3′ (reverse); *AciI* RFLP, 5′-CAATAGA TAAAGGCAAAGAGA-3′ (forward) and 5′-GAAAGACTG CTGTAGGAAAAA-3′ (reverse); *AfaI* RFLP, 5′-GCAGTG TTCTCTCCTTCATTATGTA-3′ (forward) and 5′-CTAT GTTTCTTTCTTTTTCTTTTCA-3′ (reverse). All PCR products contain either a *Hae*III or *Mbo*II restriction site. PCR was carried out under the same conditions for the screening of the variants, but only for 24–30 cycles. RFLP products were electrophoresed on a 3% agarose gel, then stained with SYBR green I (Takara). The relative expression of each allele was quantified on the basis of the difference in band intensities between the two alleles with a fluorescence image analyzer (Hitachi, Tokyo, Japan) using Analysis Version 6.0 software. As a control, genomic DNA PCR–RFLP products were included and ratios of the allele-specific band intensities were taken as a 1 : 1 allelic representation. In order to eliminate sampling or measurement error, we conducted the experiment for each sample with three replicates.

Methylation analysis

The methylation status of the CpG island which is ~30 kb upstream of the translational start codon (nt 36441–36896, GenBank accession no. AF280107), was confirmed by the bisulfite sequencing method (52). DNA was treated with sodium bisulfite using a CpGenome DNA modification kit (Intergen, Purchase, NY, USA) according to the manufacturer's instructions. PCR was performed in a total volume of 25 μl consisting of 50 ng of bisulfite modified genomic DNA, 0.625 U of DNA polymerase and 0.25 μM of each primer; 5′-GGGTTTTATTTAGTTTGAGTTT-3′ (forward) and 5′-TAACCCCTCCTCTACATTCTAT-3′ (reverse). After an initial denaturation at 95°C for 9 min, 43 cycles of 40 s at 95°C, 45 s at 52°C and 1 min at 72°C, as well as a final extension for 5 min at 72°C, were performed. The PCR product was cloned into the pGEM-T easy vector (Promega, Madison, WI, USA) then transformed into JM-109 (Promega), and plasmid DNA was collected by QIAprep Spin Mini-prep kit (Qiagen,). The CpG methylation status of individual DNA strands was determined on the basis of a comparison with the sequence obtained from the genomic DNA without the addition of bisulfite modifications. Percent methylation of each site was determined by dividing the number of methylated CpGs at a specific site by the total number of clones analyzed ($n = 20$ in all cases).

Quantitative real-time PCR

Quantification of total hepatic CYP3A4 mRNA and hnRNA was performed by real-time PCR detection using an ABI PRISM 7700 sequence detector (Applied Biosystems) with SYBR green detection of amplification products. Amplification mixtures contained 12.5 μl of 2 × SYBR green I Universal PCR Mix (Applied Biosystems), 0.5 μl of cDNA synthesis mixture, 5 pmol each of the forward and reverse primers and distilled water in a total volume of 25 μl. All primers were designed using the PrimerExpress program (Applied Biosystems). Primers for CYP3A4 mRNA were directed to a sequence that spans the junction of exons 12 and 13, corresponding to open reading frame 1405–1465; 5′-AAAGAAAC ACAGATCCCCCTGAA-3′ (forward) and 5′-CGGGTTTTTC TGGTTGAAGAAGT-3′ (reverse). CYP3A4 hnRNA primers were directed to a sequence located at bases +2253 to +2351 within intron 12 of the *CYP3A4* gene sequence; 5′-CACAGG TTTCCATGAATTTGTCT-3′ (forward) and 5′-AAGATTGG ACAGTGAGAGCATTC-3′ (reverse). The copy number of the transcript was measured against a copy-number standard curve of cloned target templates consisting of serial 10-fold dilution points. β_2-Microglobulin mRNA was used as the reference message for both CYP3A4 mRNA and hnRNA.

Testosterone 6β-hydroxylation capability in human liver samples

All incubations were performed in duplicate in solutions containing potassium phosphate (0.1 M, pH 7.4) and human liver microsomes (0.05 mg). Testosterone (final concentration, 30 μM) was added to the incubation mixture at a final methanol concentration of 1%, and the mixtures were incubated at 37°C for 10 min. We added a NADPH-generating system to initiate the reaction. Reactions were terminated by the addition of 100 μl of ice-CH_3CN. We used high-performance liquid chromatography (HPLC) to measure the quantities of extracted compounds (53).

ACKNOWLEDGEMENTS

This study was supported by RR2002, Grant-in-Aid for Scientific Research from the Ministry of Education, Culture, Sports and Technology, and Health and Labour Science Research Grants (Research on Advanced Medical Technology) from The Ministry of Health, Labour and Welfare, Tokyo, Japan.

REFERENCES

1. Thummel, K.E. and Wilkinson, G.R. (1998) *In vitro* and *in vivo* drug interactions involving human CYP3A. *Annu. Rev. Pharmacol. Toxicol.*, **38**, 389–430.
2. Li, A.P., Kaminski, D.L. and Rasmussen, A. (1995) Substrates of human hepatic cytochrome P450 3A4. *Toxicology*, **104**, 1–8.
3. Evans, W.E. and Relling, M.V. (1999) Pharmacogenomics: translating functional genomics into rational therapeutics. *Science*, **286**, 487–491.
4. Shimada, T., Yamazaki, H., Mimura, M., Inui, Y. and Guengerich, F.P. (1994) Interindividual variations in human liver cytochrome P-450 enzymes involved in the oxidation of drugs, carcinogens and toxic chemicals: studies with liver microsomes of 30 Japanese and 30 Caucasians. *J. Pharmacol. Exp. Ther.*, **270**, 414–423.

5. Lown, K.S., Thummel, K.E., Benedict, P.E., Shen, D.D., Turgeon, D.K., Berent, S. and Watkins, P.B. (1995) The erythromycin breath test predicts the clearance of midazolam. *Clin. Pharmacol. Ther.*, **57**, 16–24.
6. Ozdemir, V., Kalowa, W., Tang, B.K., Paterson, A.D., Walker, S.E., Endrenyi, L. and Kashuba, A.D. (2000) Evaluation of the genetic component of variability in CYP3A4 activity: a repeated drug administration method. *Pharmacogenetics*, **10**, 373–388.
7. Rebbeck, T.R., Jaffe, J.M., Walker, A.H., Wein, A.J. and Malkowicz, S.B. (1998) Modification of clinical presentation of prostate tumors by a novel genetic variant in CYP3A4. [Erratum (1999) *J. Natl Cancer. Inst.*, **91**, 1082.] *J. Natl Cancer. Inst.*, **90**, 1225–1229.
8. Ball, S.E., Scatina, J., Kao, J., Ferron, G.M., Fruncillo, R., Mayer, P., Weinryb, I., Guida, M., Hopkins, P.J., Warner, N. *et al.* (1999) Population distribution and effects on drug metabolism of a genetic variant in the 5′ promoter region of CYP3A4. *Clin. Pharmacol. Ther.*, **66**, 288–294.
9. Westlind, A., Lofberg, L., Tindberg, N., Andersson, T.B. and Ingelman-Sundberg, M. (1999) Interindividual differences in hepatic expression of CYP3A4: relationship to genetic polymorphism in the 5′-upstream regulatory region. *Biochem. Biophys. Res. Commun.*, **259**, 201–205.
10. Sata, F., Sapone, A., Elizondo, G., Stocker, P., Miller, V.P., Zheng, W., Raunio, H., Crespi, C.L. and Gonzalez, F.J. (2000) CYP3A4 allelic variants with amino acid substitutions in exon 7 and 12: evidence for an allelic variant with altered catalytic activity. *Clin. Pharmacol. Ther.*, **67**, 48–56.
11. Wandel, C., Witte, J.S., Hall, J.M., Stein, C.M., Wood, A.J. and Wilkinson, G.R. (2000) CYP3A activity in African American and European American men: population differences and functional effect of the CYP3A4*1B5′-promoter region polymorphism. *Clin. Pharmacol. Ther.*, **68**, 288–294.
12. Eiselt, R., Domanski, T.L., Zibat, A., Mueller, R., Presecan-Siedel, E., Hustert, E., Zanger, U.M., Brockmoller, J., Klenk, H.P., Meyer, U.A. *et al.* (2001) Identification and functional characterization of eight CYP3A4 protein variants. *Pharmacogenetics*, **11**, 447–458.
13. Brannan, C.I. and Bartolomei, M.S. (1999) Mechanisms of genetic imprinting. *Curr. Opin. Genet. Dev.*, **9**, 164–170.
14. Constancia, M., Pickard, B., Kelsey, G. and Reik, W. (1998) Imprinting mechanisms. *Genet. Res.*, **8**, 881–900.
15. Cooper, D.W., Johnston, P.G., Watson, J.M. and Graves, J.A.M. (1993) X-inactivation in marsurpials and monotremes. *Semin. Dev. Biol.*, **4**, 117–128.
16. Yan. H., Yuan, W., Velculescu, V.E., Vogelstein, B. and Kinzler, K.W. (2002) Allelic variation in human gene expression. *Science*, **297**, 1143.
17. Pastinen, T., Sladek, R., Gurd, S., Sammak, A., Ge, B., Lepage, P., Lavergne, K., Villeneuve, A., Gaudin, T., Brandstrom, H. *et al.* (2004) A survey of genetic and epigenetic variation affecting human gene expression. *Physiol. Genomics*, **16**, 184–193.
18. Horike, S., Mitsuya, K., Meguro, M., Kotobuki, N., Kashiwagi, A., Notsu, T., Schulz, T.C., Shirayoshi, Y. and Oshimura, M. (2000) Targeted disruption of the human LIT1 locus defines a putative imprinting control element playing as essential role in Beckwith–Weidemann syndrome. *Hum. Mol. Genet.*, **9**, 2075–2083.
19. Brooks, B.A., McBride, O.W., Dolphin, C.T., Farrall, M., Scambler, P.J., Gonzalez, F.J. and Idle, J.R. (1988) The gene *CYP3* encoding P450pcn1 (nifedipine oxidase) is tightly linked to the gene *COL1A2* encoding collagen type 1 alpha on 7q21–q22.1. *Am. J. Hum. Genet.*, **43**, 280–284.
20. Spurr, N.K., Gough, A.C., Stevenson, K. and Wolf, C.R. (1989) The human cytochrome P450 CYP3 locus: assignment to chromosome 7q22–qter. *Hum. Genet.*, **81**, 171–174.
21. Okita, C., Meguro, M., Hoshiya, H., Haruta, M., Sakamoto, Y.K. and Oshimura, M. (2003) A new imprinted cluster on the human chromosome 7q21–q31, identified by human–mouse monochromosomal hybrids. *Genomics*, **81**, 556–559.
22. Lo, H.S., Wang, Z., Hu, Y., Yang, H.H., Gere, S., Buetow, K.H. and Lee, M.P. (2003) Allelic variation in gene expression is common in the human genome. *Genome Res.*, **13**, 1855–1862.
23. Reik, W. and Walter, J. (1998) Imprinting mechanisms in mammals. *Curr. Opin. Genet. Dev.*, **8**, 154–164.
24. Tilghman, S.M. (1999) The sins of the fathers and mothers: genomic imprinting in mammalian development. *Cell*, **96**, 185–193.
25. Evans, H.K., Wylie, A.A., Murphy, S.K. and Jirtle, R.L. (2001) The neuronatin gene resides in a 'micro-imprinted' domain on human chromosome 2–q11.2. *Genomics*, **77**, 99–104.
26. Kuehl, P., Zhang, J., Lin, Y., Lamba, J., Assem, M., Schuetz, J., Watkins, P.B., Daly, A., Wrighton, S.A., Hall, S.D. *et al.* (2001) Sequence diversity in CYP3A promoters and characterization of the genetic basis of polymorphic CYP3A5 expression. *Nat. Genet.*, **27**, 383–391.
27. Tirona, R.G., Lee, W., Leake, B.F., Lan, L.B., Cline, C.B., Lamba, V., Parviz, F., Duncan, S.A., Inoue, Y., Gonzalez, F.J., Schuetz, E.G. and Kim, R.B. (2003) The orphan nuclear receptor HNF4alpha determines PXR- and CAR-mediated xenobiotic induction of CYP3A4. *Nat. Med.*, **9**, 220–224.
28. Goodwin, B., Hodgson, E. and Liddle, C (1999) The orphan human pregnane X receptor mediates the transcriptional activation of CYP3A4 by rifampicin through a distal enhancer module. *Mol. Pharmacol.*, **56**, 1329–1339.
29. Johnson, R.F., Mitchell, C.M., Giles, W.B., Walters, W.A. and Zakar, T. (2002) The *in vivo* control of prostaglandin H synthase-2 messenger ribonucleic acid expression in the human amnion at parturition. *Clin. Endocrinol. Metab.*, **87**, 2816–2823.
30. Johnson, R.F., Mitchell, C.M., Giles, W.B., Walters, W.A. and Zakar, T. (2003) The control of prostaglandin endoperoxide H-synthase-2 expression in the human chorion laeve at term. *J. Soc. Gynecol. Investig.*, **10**, 222–230.
31. Weber, M., Hagege, H., Lutfalla, G., Dandolo, L., Brunel, C., Cathala, G. and Forne, T. (2003) A real-time polymerase chain reaction assay for quantification of allele ratios and correction of amplification bias. *Anal. Biochem.*, **320**, 252–258.
32. Hsieh, K.P., Lin, Y.Y., Cheng, C.L., Lai, M.L., Lin, M.S., Siest, J.P. and Huang, J.D. (2001) Novel mutations of *CYP3A4* in Chinese. *Drug Metab. Dispos.*, **29**, 268–273.
33. Eap, C.B., Buclin, T., Hustert, E., Bleiber, G., Golay, K.P., Aubert, A.C., Baumann, P., Telenti, A. and Kerb, R. (2004) Pharmacokinetics of midazolam in *CYP3A4*- and *CYP3A5*-genotyped subjects. *Eur. J. Clin. Pharmacol.*, **60**, 231–236.
34. Garcia-Martin, E., Martinez, C., Pizarro, R.M., Garcia-Gamito, F.J., Gullsten, H., Raunio, H. and Agundea, J.A. (2002) *CYP3A4* variant alleles in white individuals with low CYP3A4 enzyme activity. *Clin. Pharmacol. Ther.*, **71**, 196–204.
35. Mitsuya, K., Sui, H., Meguro, M., Kugoh, H., Jinno, Y., Niikawa, N. and Oshimura, M. (1997) Paternal expression of *WT1* in human fibroblasts and lymphocytes. *Hum. Mol. Genet.*, **6**, 2243–2246.
36. Jinno, Y., Yun, K., Nishiwaki, K., Kubota, T., Ogawa, O., Reeve, A.E. and Niikawa, N. (1994) Mosaic and polymorphic imprinting of the *WT1* gene in humans. *Nat. Genet.*, **6**, 305–309.
37. Nishiwaki, K., Niikawa, N. and Ishikawa, M. (1997) Polymorphic and tissue-specific imprinting of the human Wilms tumor gene, *WT1*. *Jpn J. Hum. Genet.*, **42**, 205–211.
38. Schweifer, N., Valk, P.J., Delwel, R., Cox, R., Francis, F., Meier-Ewert, S., Lehrach, H. and Barlow, D.P. (1997) Characterization of the C3 YAC contig from proximal mouse chromosome 17 and analysis of allelic expression of genes flanking the imprinted *Igf2r* gene. *Genomics*, **43**, 285–297.
39. Dao, D., Frank, D., Qian, N., O'Keefe, D., Vosatka, R.J., Walsh, C.P. and Tycko, B. (1998) *IMPT1*, an imprinted gene similar to polyspecific transporter and multi-drug resistance genes. *Hum. Mol. Genet.*, **7**, 597–608.
40. Sy, S.K., Ciaccia, A., Li, W., Roberts, E.A., Okey, A., Kalow, W. and Tang, B.K. (2002) Modeling of human hepatic CYP3A4 enzyme kinetics, protein, and mRNA indicates deviation from log-normal distribution in *CYP3A4* gene expression. *Eur. J. Clin. Pharmacol.*, **58**, 357–365.
41. Gonzales, F. and Lee, Y. (1996) Constitutive expression of hepatic cytochrome P450 genes. *FASEB J.*, **10**, 1112–1117.
42. Wang, J.C., Stafford, J.M., Scott, D.K., Sutherland, C. and Granner, D.K. (2000) The molecular physiology of hepatic nuclear factor 3 in the regulation of gluconeogenesis. *J. Biol. Chem.*, **275**, 14717–14721.
43. Ourlin, J.C., Jounaidi, Y., Maurel, P. and Vilarem, M.J. (1997) Role of the liver-enriched transcription factors C/EBP alpha and DBP in the expression of human *CYP3A4* and *CYP3A7*. *J. Hepatol.*, **26** (Suppl. 2), 54–62.
44. Rodriguez-Antona, C., Bort, R., Jover, R., Tindberg, N., Ingelman-Sundberg, M., Gomez-Lechon, M.J. and Castell, J.V. (2003) Transcriptional regulation of human *CYP3A4* basal expression by CCAAT enhancer-binding protein alpha and hepatocyte nuclear factor-3 gamma. *Mol. Pharmacol.*, **63**, 1180–1189.

45. Burk, O. and Wojnowski, L. (2004) Cytochrome P450 3A and their regulation. Naunyn. Schmiedebergs. *Arch. Pharmacol.*, **369**, 105–124.
46. Yan, H. and Zhou, W. (2004) Allelic variations in gene expression. *Curr. Opin. Oncol.*, **16**, 39–43.
47. Hardison, R.C., Oeltjen, J. and Miller, W. (1997) Long human–mouse sequence alignments reveal novel regulatory elements: a reason to sequence the mouse genome. *Genome Res.*, **7**, 959–966.
48. Jaenisch, R. and Bird, A. (2003) Epigenetic regulation of gene expression: how the genome integrates intrinsic and environmental signals. *Nat. Genet.*, **33**, S245–S254.
49. Sleutels, F., Zwart, R. and Barlow, D.P. (2002) The non-coding Air RNA is required for silencing autosomal imprinted genes. *Nature*, **415**, 810–813.
50. Finta, C. and Zaphiropoulos, P.G. (2000) The human cytochrome P450 3A locus. Gene evaluation by capture of downstream exons. *Gene*, **260**, 13–23.
51. Wojnowski, L. and Brockmoller, J. (2004) Single nucleotide polymorphism characterization by mRNA expression imbalance assessment. *Pharmacogenetics*, **14**, 267–269.
52. Frommer, M., McDonald, L.E., Millar, D.S., Collis, C.M., Watt, F., Grigg, G.W., Molloy, P.L. and Paul, C.L. (1992) A genomic sequencing protocol that yields a positive display of 5-methylcytosine residues in individual DNA strands. *Proc. Natl Acad. Sci. USA*, **89**, 1827–1831.
53. Yoshimoto, K., Echizen, H., Chiba, K., Tani, M. and Ishizaki, T. (1995) identification of human CYP isoforms involved in the metabolism of propranolol enantiomers-*N*-desisopropylation is mediated mainly by CYP1A2. *Br. J. Clin. Pharmacol.*, **39**, 421–431.

MUTATION IN BRIEF

Novel *TSC2* Mutations and Decreased Expression of Tuberin in Cultured Tumor Cells with an Insertion Mutation

Jian-Hua Feng[1,2], Toshiyuki Yamamoto[3]*, Eiji Nanba[3], Haruaki Ninomiya[4], Akira Oka[2], and Kousaku Ohno[2]

[1]Department of Child Neurology, Children Hospital, Zhejiang University, Hangzhou, P.R. China; [2]Division of Child Neurology, Institute of Neurological Sciences, Faculty of Medicine, Tottori University, Yonago, Japan; [3]Gene Research Center, Tottori University, Yonago, Japan; [4]Department of Neurobiology, School of Life Sciences, Faculty of Medicine, Tottori University, Yonago, Japan

*Correspondence to: Toshiyuki Yamamoto, M.D., Ph.D., Division of Medical Genetics, Kanagawa Children's Medical Center (KCMC), 2-138-4 Mutsukawa, Minami-ku, Yokohama 232-8555, Japan; Tel.: +81-45-711-2351; Fax: +81-45-742-7821; E-mail: nikau@basil.freemail.ne.jp

Grant sponsor: The Ministry of Health, Labour and Welfare of Japan, and the Ministry of Education, Culture, Sports, Science and Technology of Japan

Communicated by Mark H. Paalman

Tuberous sclerosis complex (TSC) is an autosomal dominant disorder characterized by hamartomas in many organs. Two genes responsible for TSC, *TSC1* and *TSC2*, were recently identified. *TSC1* and *TSC2* encode the proteins hamartin and tuberin, respectively, and 337 different mutations have been reported in these genes thus far. Here, we report six novel *TSC2* mutations including one missense mutation, two nonsense point mutations, two frameshifts, and an insertion mutation. The insertion mutation is unique because of its location at an exon/intron boundary that results in triplication of a 34-bp sequence. Cultured tumor cells from the patient with this insertion mutation exhibited a decreased level of tuberin as revealed by Western blotting, suggesting that the mRNA of *TSC2* is not translated as efficiently or the translated protein exhibits reduced stability. Five novel polymorphisms of *TSC2* were also identified. As previously reported, the missense mutations were located in the GTPase activating protein-related domain of *TSC2* encoded in exons 34-38. No *TSC1* mutations were identified in the present subjects. © 2004 Wiley-Liss, Inc.

KEY WORDS: giant cell astrocytoma; Japanese; mutation; *TSC2*; tuberin; tuberous sclerosis complex

INTRODUCTION

Tuberous sclerosis complex (TSC) (MIM# 191100) is an autosomal dominant disorder characterized by the development of hamartomatous growth in many different organs, most commonly in the brain, heart, kidney and skin (Gomez et al., 1999). Involvement of the brain is associated with the most problematic clinical manifestations

Received 26 August 2003; accepted revised manuscript 22 January 2004.

DOI: 10.1002/humu.9225

of TSC, including intellectual handicap, epilepsy and abnormal behavior (Cheadle et al., 2000). Approximately two-thirds of the cases are sporadic, without family history, reflecting a high spontaneous mutation rate in the underlying genes (Osborne et al., 1991, Sampson et al., 1994).

Two TSC-related genes were previously identified by positional cloning. *TSC2* (MIM# 191092) is located on chromosome 16p13.3 and consists of 41 exons, whereas *TSC1* (MIM# 191100) is located on 9q34 and consists of 23 exons (The European Chromosome 16 Tuberous Sclerosis Consortium 1993; van Slegtenhorst et al., 1997). *TSC2* encodes the 200-kDa protein tuberin that contains a GTPase activating protein (GAP)-related domain (The European Chromosome 16 Tuberous Sclerosis Consortium 1993). Hamartin, the 130-kDa predicted product of *TSC1*, is a novel protein that is predicted to form a complex with tuberin (van Slegtenhorst et al., 1997). Loss of heterozygosity (LOH) of either *TSC1* or *TSC2* in affected tissues indicates that each acts as a tumor suppressor (Green et al., 1994; Henske et al., 1995; Sepp et al., 1996).

At least, 131 and 343 different disease causing mutations have been reported in *TSC1* and *TSC2*, respectively (Cheadle et al., 2000; The Human Gene Mutation Database at the Institute of Medical Genetics in Cardiff http://archive.uwcm.ac.uk/uwcm/mg/hgmd0.html). Here, we used single-strand conformational polymorphism (SSCP) analysis of genomic DNA to identify six novel mutations in Japanese TSC patients. Tuberin expression was decreased in cultured tumor cells from a patient with a unique insertion mutation in *TSC2*.

MATERIALS AND METHODS

Patients

Clinical information for all patients is summarized in Table 1. Patient 1 was a 9-year-old female. Her early developmental milestones were normal. She suffered from febrile convulsions at age 2, and at age 5 was diagnosed with TSC due to sebacea and brain calcifications revealed by computed tomography (CT). At 6 years of age, she presented with afebrile convulsions, and electroencephalography (EEG) revealed right parietal focal spikes and waves. Her mental milestones indicated mild retardation.

Table 1. Summary of the Clinical Information of the Patients

Patient	Age	Gender	Skin	Neurological Findings	Brain Radiological Findings	Others
Patient 1 (s)	9	F	+	seizures, mild MR	calcification	
Patient 2 (nd)	20	M	+	seizures, severe MR	?	bilateral renal tumor
Patient 3 (f)	15	F	+	seizures, MR	+ (no detailed information)	bilateral renal tumor, lung lymphangima
Patient 4 (nd)	16	F	?	(normal intelligence)	calcification	left renal tumor
Patient 5 (s)	1	M	+	West, mild developmental delay	PN, CD, heterotopia	cardiac tumor
Patient 6 (s)	2	F	+	West	PN, CD, heterotopia	cardiac tumor
Patient 7 (f)	15	F	+	West to Lennox, severe MR	PN, tubers	cardiac tumor
Patient 8 (f)	24	F	+	West syndrome, moderate MR	PN, calcification	brain tumor
Patient 9 (s)	2	F	+	seizures	calcification	
Patient 10 (s)	7	F	+	West syndrome	PN, tubers	

skin, skin involvement; s, sporadic case; f, familial case; nd, not detected; F, female; M, male; ?, unknown

MR, mental retardation; PN, periventricular nodules; CD, cortical dysplasia

Patient 2 was a 20-year-old male. At 10 months of age, he suffered febrile convulsions and was diagnosed with a developmental delay. At 17 months of age, a left renal tumor was surgically removed, the pathological diagnosis of which was renal cell carcinoma. At age 17 years, right renal angiolipoma was identified. His mental state was one of severe retardation, and he displayed white skin patches.

Patient 3 was a 15-year-old girl. In infancy, she suffered from seizure attacks and subsequently exhibited delayed psychomotor development. Periventricular nodules were noted by radiological examination. White skin

patches were also noted. At 13 years of age, bilateral renal angiolipomas were identified and surgically removed. At age 14, she had a first incidence of spontaneous pneumothorax with recurrent episodes in subsequent years. A chest X-ray revealed bilateral lung cystic lesions that were suspected to be lymphangiomas.

Patient 4 was a 16-year-old girl. At age 3 months, a right renal tumor was surgically removed and found to be cystic dysplasia. Her first epileptic episode occurred at age 1 year. At present, she has normal intelligence in spite of brain calcification. She has no cystic lesions in her left kidney but has an angiomyolipoma in the liver.

Patient 5 was the second child of healthy parents, and was immediately diagnosed with multiple cardiac tumors just after delivery. At 1 month of age, he presented with white skin patches and developed tonic spasms. Brain CT showed periventricular nodules and MRI showed left fronto-parietal cortical dysplasia and heterotopia. Now, at 1 year of age, he exhibits mild developmental delay.

Patient 6 was a 2-year-old girl. At 4 months of age, she was afflicted with infantile spasms, and an EEG indicated hypsarhythmia. She had white skin patches and cardiac rhabdomyoma that was identified by echocardiography. Brain MRI showed small nodules in periventricular regions.

Patient 7 was a 15-year-old girl. Although her parents were healthy, her younger brother had retinal hamartomas. She had white patches, facial angiofibromas and ungual fibroma. Radiological findings suggested subependymal nodules and tubers in the brain and cardiac rhabdomyoma. In infancy, she had West syndrome that later developed into Lennox syndrome. Her present intelligence quotient (I.Q.) is below 20.

Patient 8 was a 24-year-old female. At age 11 months she suffered infantile spasms. Many white spots were present on her skin. Brain radiological examinations revealed a right anterior ventricular tumor and periventricular calcifications. When she was 8 months old, she had chronic left facial palsy that may have been related to a tumor, and her symptoms disappeared after resection of a tumor that was diagnosed as a giant cell astrocytoma (cells were cultured from the resected tumor tissues, and were used for Western blotting). Presently, she exhibits moderate mental retardation. Although her parents and an elder sister are healthy, her father has white macules.

Patient 9 was a 2-year-old girl. Following her first epileptic attack, a detailed investigation suggested TSC based on white macules and brain calcifications.

Patient 10 was a 7-year-old boy that displayed white macules. He developed West syndrome at 5 months of age. Radiological examination showed periventricular nodules and some tubers. Presently, he shows moderate mental retardation. His parents are healthy.

Molecular analysis

DNAs were extracted from peripheral lymphocytes using a standard method. Sixty-four normal control DNAs were also obtained from blood samples of healthy Japanese volunteers and used for a population study. Informed consent for genomic examinations was obtained from all patients and volunteers. The Caucasian Population Panel 100 was provided by the Coriell Institute for Medical Research (NJ, USA) and fifty DNAs samples were used for population study. Polymerase chain reaction (PCR) was used to amplify all exons of *TSC1* (GenBank accession number AF013168.1) and *TSC2* (GenBank accession number X75621.1) from genomic DNAs using standard methods with primers described elsewhere (Zhang et al., 1999; Pipo et al., 2000; Yamamoto et al., 2002). The PCR products were subjected to SSCP analysis using a minigel (10 cm X 10 cm). The samples were analyzed under four different electrophoresis conditions from a combination of two sets of gel mixtures (12% polyacrylamide gel with or without 5% (w/v) glycerol) and two temperatures (4°C or 22°C) (Zhang et al., 1999). DNA bands were visualized by silver staining. The PCR products that gave aberrant bands during the SSCP analysis were sequenced directly using the BigDye terminator cycle sequencing kit (Applied Biosystems, CA, USA) and the ABI PRISM 3100 genetic analyzer (Applied Biosystems). Each PCR product was sequenced in both directions using PCR primers.

Western blotting

Tumor cells of patient 8 were cultured from the resected tumor tissues, and harvested and homogenized by sonication in buffer (10 mM Tris-HCl pH 7.4, 150 mM NaCl, 1 mM EDTA, 1 mM EGTA) supplemented with 1% (w/v) Triton X-100 and protease inhibitor cocktail (Boehringer Ingelheim, Ingelheim, Germany). The suspensions were centrifuged at 12,000 x g for 30 min at 4°C and the protein concentration of the supernatant was determined by the BCA protein assay (Bio-Rad, CA, USA). Protein (10 μg) was subjected to SDS-polyacrylamide gel

electrophoresis on a 10% gel, and the proteins were electrophoretically transferred to an Immobilon membrane (Millipore, Bedford, MA). Following a 1-h preincubation in 5% (w/v) skim milk, the membrane was incubated overnight at 4°C with the tuberin antibody, tuberin (C-20) (cat. # sc-893; Santa Cruz Biotechnology, Inc., USA; diluted 1:1000). Tuberin bands were detected using avidin-biotin-alkaline phosphatase (Vector ABC-AP kit).

RESULTS AND DISCUSSION

Table 2. Summary of the Disease-Causing *TSC2* Mutations

Patient	Location	Nucleotide Change*	Amino Acid Change	Type	Novel or Reported by
Patient 1 (s)	ex4	c.469G>T	p.E157X	nonsense	novel
Patient 2 (nd)	ex19	c.2163del G		frameshift	novel
Patient 3 (f)	ex24	c.2767_2768insC		frameshift	novel
Patient 4 (nd)	ex28	c.3355C>T	p.Q1119X	nonsense	novel
Patient 5 (s)	ex37	c.4952A>G	p.N1651S	missense	Maheshwar et al., 1997
Patient 6 (s)	ex37	c.4958C>T	p.S1653F	missense	novel
Patient 7 (f)	ex38	c.5024C>T	p.P1675L	missense	Maheshwar et al., 1997
Patient 8 (f)	IVS38	c.5068+20_5068+21ins34		splicing?	novel
Patient 9 (s)	ex40	c.5238_5255del	p.H1746_R1751del	deletion	Beauchamp et al., 1998
Patient 10 (s)	ex40	c.5238_5255del	p.H1746_R1751del	deletion	Beauchamp et al., 1998

s, sporadic case; c., complementary DNA No.; f, familial case; del, deletion; ins, insertion

*GenBank X75621.1. Nucleotide numbering, with A of the initiator ATG as +1

The mutation nomenclature according to the website (http://www.HGVS.org/mutnomen/).

Six novel and three previously known mutations of *TSC2* (Table 2) were identified. All of the patients exhibited mutations in *TSC2* only, and no *TSC1* mutations were identified despite the comprehensive screening of both genes. Two new nonsense mutations and two new frameshift mutations resulted from respective deletion and insertion of 1 bp would be definitely disease causing.

A novel missense mutation within exon 37, complementary DNA No. c.4958C>T (p.S1653F) in patient 6 was not found in healthy control subjects (64 Japanese and 50 Caucasians) suggesting that they are pathogenic for TSC. The known missense mutation, c.5024C>T (p.P1675L) within exon 38 in patient 7, was recurrent and thus represents a relatively common mutation (Beauchamp et al., 1998; Zhang et al., 1999). Interestingly, all three patients (patients 5, 6 and 7) with missense mutations presented with cardiorhabdomyoma. As reported elsewhere, these missense mutations were located in the GAP-related domain of *TSC2* encoded in exons 34-38 (Cheadle et al., 2000). None of the mutations were located in the sequence CpG, a dinucleotide sequence in which nucleotide alterations are prevalent.

Interestingly, both patient 2 and 3 having a novel frameshift mutation had renal cancers, and patient 3 also suffered from lung lesions. TSC with lung lesions is relatively rare and constitutes a distinct subset of the disease termed pulmonary TSC (Kalassian et al., 1997; Sullivan 1998). A common pulmonary lesion is a parenchymal cyst that is often associated with dyspnea or pneumothorax. Typically, patients with pulmonary TSC are women of childbearing age whose pulmonary lesions may be influenced by hormonal changes (Kalassian et al., 1997; Sullivan 1998).

An 18-bp deletion (c.5238_5255del) was identified within exon 40 in both sporadic patients 9 and 10. As this in-frame deletion has been frequently identified in TSC patients (Dabora et al., 2001), this region may constitute a hot spot. Another 18-bp in-frame deletion, c.5256_5273del (adjacent to 18-bp deletion at c. 5238_5255) was also identified frequently in four unrelated sporadic cases (Jones et al., 1999). These deletions occur in the sequence context of a direct repeat of eleven nucleotides with seven intervening nucleotides, and are likely the product of

slipped mispairing during replication (Cooper and Krawczak 1991). The recurrent 18-bp deletion in exon 40 of *TSC2* lies within the putative rabaptin-binding domain (Xiao et al., 1997).

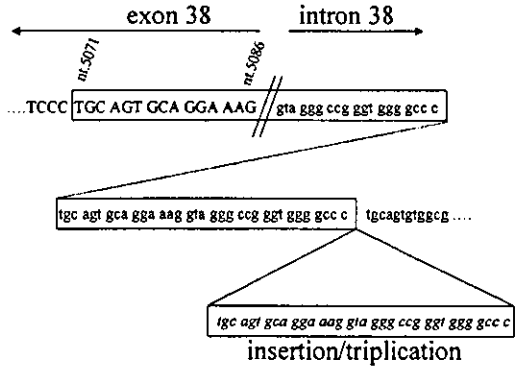

Figure 1. Schematic representation of the sequence around the site of the insertion detected in patient 8. Open boxes indicate the set of 34-bp sequences that is duplicated in the normal sequence and triplicated in patient 8. Uppercase and lowercase nucleotides indicate exonic and intronic sequences, respectively.

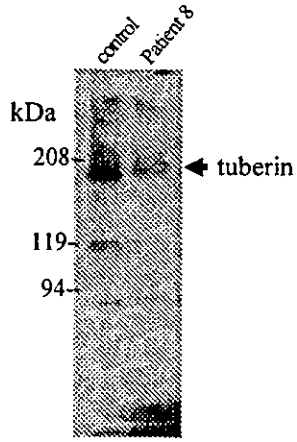

Figure 2. Western blot analysis. It was confirmed that the same amount of protein had been loaded in each lane and transferred by staining gel and unused portion of membrane with Coomassie brilliant blue (data not shown). The arrowhead indicates tuberin, the expression of which is decreased in the sample from patient 8 compared with that of control. The migration of molecular weight markers is shown to the left. C, control sample derived from an autopsied brain.

A 34-bp insertion (c.5068+20_5068+21ins34) was identified in patient 8. In the normal genomic sequence, this 34-bp sequence (TGC AGT GCA GGA AAG GTA GGG CCG GGT GGG GCC C) is duplicated across the boundary of exon 38 and intron 38 (Fig. 1). Patient 8 had three repeats of this 34-bp sequence and there was no other mutation in any of the exons of *TSC1* and *TSC2*. This patient was a familial case, but attempts to obtain samples from family members were unsuccessful. Thus, to exclude the possibility that the triplication represented benign polymorphisms, we analyzed this region in normal Japanese controls as well as in the Caucasian Population Panel 100. As expected, this duplication was not observed in any of the control samples. To test whether this insertion influences pre-mRNA splicing, cDNA was analyzed around this exon 38 using reverse-transcription PCR. However, no aberrant splicing was observed (data not shown). To estimate the impact of this genomic mutation, tuberin expression was assessed in primary-cultured cells from the patient's giant cell astrocytoma.

Tuberin expression was decreased compared with normal brain tissue (Fig. 3). This result is compatible with mutational loss of *TSC2* (Wienecke et al., 1997). However, we cannot exclude the possibility that secondary effects such as hamartin or rap1 expression may negatively influence tuberin expression.

Unlike many other symptoms that show age-dependant penetration, intellectual disability in TSC is almost invariably present from early childhood and rarely escapes detection. However, patient 4 (carrying a nonsense mutation) exhibited normal intellectual development. Patients 9 and 10 carried the same mutation, but their clinical features were different from one other. Thus, the extent of the protein truncation expected from mutations in *TSC2* does not necessarily correlate with the severity of the clinical symptoms. Therefore, the severity is likely dependent on other somatic mutations within the pathogenic lesions. Future determination of the pathogenesis of these genomic mutations will require the development of a functional assay for tuberin activity.

Five novel variations of *TSC2* were also identified (Table 3). The each variation was coincidentally identified in only one control sample which was used for population study. Thus, these variation would be very rare and not disease causing.

Table 3. Summary of the *TSC2* Polymorphisms

Location	Nucleotide change*	Amino Acid Change	Type	Novel or Reported by	Frequency#
ex14	c.1593C>T	p.I531	silent	Yamashita et al., 2000	
ex16	c.1819G>A	p.A607T	missense	novel	1/114
ex22	c.2585C>T	p.A862V	missense	novel	1/114
ex33	c.4285G>T	p.A1429S	minsense	novel	1/114
ex33	c.4349C>G	p.P1450R	missense	novel	1/114
IVS33	c.4493+17C>T			novel	1/114
IVS39	c.5161-9C>A			Jones et al., 1999	
ex40	c.5202T>C	p.D1734	silent	Au et al., 1997	
ex41 (3' non-coding region)	c.5424+55_5424+58delTAAA			Kumar et al., 1995	

c., complementary DNA No.; *GenBank X75621.1. Nucleotide numbering, with A of the initiator ATG as +1

#Frequency of each variation was described as 1/114, because the each variation was detected in only one sample among 64 healthy Japanese volunteers and 50 samples of Caucasian DNA panel.

ACKNOWLEDGMENTS

This work was supported by the Ministry of Health, Labour and Welfare of Japan through a special grant for neurocutaneous disease, and by the Ministry of Education, Culture, Sports, Science and Technology of Japan with a grant in aid of scientific research. We are grateful to Dr. Mitsuhiro Kato, Takashi Shiihara (Yamagata Univ.), Dr. Masako Kubo (Yamanashi Prefectural Central Hospital), Dr. Atsushi Iwao, Dr. Masamune Higashikawa (Yamada Red Cross Hospital), Dr. Akihisa Okumura (Nagoya Univ.), Dr. Masashi Mizuguchi (Jichi Medical Scholl) and Dr. Nobuaki Iwasaki (Tsukuba Univ.) for their support.

REFERENCES

Au KS, Rodriguez JA, Rodriguez E Jr, Dobyns WB, Delgado MR, Northrup H (1997). Mutations and polymorphisms in the tuberous sclerosis complex gene on chromosome 16. Hum Mutat 9: 23-29

Beauchamp RL, Banwell A, McNamara P, Jacobsen M, Higgins E, Northrup H, Short P, Sims K, Ozelius L, Ramesh V(1998). Exon scanning of the entire TSC2 gene for germline mutations in 40 unrelated patients with tuberous sclerosis. Hum Mutat 12: 408-416

Cheadle JP, Reeve MP, Sampson JR, Kwiatkowski DJ (2000). Molecular genetic advances in tuberous sclerosis. Hum Genet 107: 97-114

Cooper DN, Krawczak M (1991). Mechanisms of insertional mutagenesis in human genes causing genetic disease. Hum Genet 87: 409-415

Dabora SL, Jozwiak S, Franz DN, Roberts PS, Nieto A, Chung A, Choy Y-S, Reeve MP, Thiele E, Egelhoff JC, Kaspirzyk-Obara J, Domanska-Pakiela D, Kwiatkowski DJ (2001). Mutational analysis in a cohort of 224 tuberous sclerosis patients indicates increased severity of TSC2, compared with TSC1, disease in multiple organs. Am J Hum Genet 68: 64-80.

Gomez MR, Sampson JR, Holets-Whittemore V (1999). Tuberous sclerosis complex, 3rd edn. New York: Oxford University Press

Green AJ, Johnson PH, Yates JR (1994). The tuberous sclerosis gene on chromosome 9q34 acts as a growth suppressor. Hum Mol Genet 3: 1833-1834

Henske EP, Neumann HP, Scheithauer BW, Herbst EW, Short MP, Kwiatkowski DJ (1995). Loss of heterozygosity in the tuberous sclerosis (TSC2) region of chromosome band 16p13 occurs in sporadic as well as TSC-associated renal angiomyolipomas. Genes Chromosomes Cancer 13: 295-298

Jones AC, Shyamsundar MM, Thomas MW, Maynard J, Idziaszczyk S, Tomkins S, Sampson JR, Cheadle JP (1999). Comprehensive mutation analysis of TSC1 and TSC2-and phenotypic correlations in 150 families with tuberous sclerosis. Am J Hum Genet 64: 1305-1315

Kalassian KG, Doyle R, Kao P, Ruoss S, Raffin TA (1997). Lymphangioleiomyomatosis: new insights. Am J Respir Crit Care Med 155: 1183-1186

Kumar A, Kandt RS, Wolpert C, Roses AD, Pericak-Vance MA, Gilbert JR (1995). Mutation analysis of the TSC2 gene in an African-American family. Hum Mol Genet 4: 2295-2298

Maheshwar MM, Cheadle JP, Jones AC, Myring J, Fryer AE, Harris PC, Sampson JR (1997). The GAP-related domain of tuberin, the product of the TSC2 gene, is a target for missense mutations in tuberous sclerosis. Hum Mol Genet 6: 1991-1996

Osborne JP, Fryer A, Webb D (1991). Epidemiology of tuberous sclerosis. Ann N Y Acad Sci 615: 125-127

Pipo JR, Yamamoto T, Takeda H, Maegawa S, Nanba E, Ninomiya H, Ohno K, Takeshita K (2000). Two novel serine repeat length polymorphisms (1043 ins S and 1043 ins SS) at exon 23 of the TSC1 gene. Hum Mutat 16: 375.

Sampson JR, Harris PC (1994). The molecular genetics of tuberous sclerosis. Hum Mol Genet 3: 1477-1480

Sepp T, Yates JR, Green AJ (1996). Loss of heterozygosity in tuberous sclerosis hamartomas. J Med Genet 33: 962-964

Sullivan EJ (1998). Lymphangioleiomyomatosis. A review. Chest 114: 1689-1703

The European Chromosome 16 Tuberous Sclerosis Consortium (1993). Identification and characterization of the tuberous sclerosis gene on chromosome 16. Cell 75: 1305-1315

van Slegtenhorst M, de Hoogt R, Hermans C, Nellist M, Janssen B, Verhoef S, Lindhout D, van den Ouweland A, Halley D, Young J, Burley M, Jeremiah S, Woodward K, Nahmias J, Fox M, Ekong R, Osborne J, Wolfe J, Povey S, Snell RG, Cheadle JP, Jones AC, Tachataki M, Ravine D, Kwiatkowski DJ, et al (1997). Identification of the tuberous sclerosis gene TSC1 on chromosome 9q34. Science 277: 805-808

Wienecke R, Guha A, Maize JC Jr, Heideman RL, DeClue JE, Gutmann DH (1997). Reduced TSC2 RNA and protein in sporadic astrocytomas and ependymomas. Ann Neurol 42: 230-235

Xiao GH, Shoarinejad F, Jin F, Golemis EA, Yeung RS (1997). The tuberous sclerosis 2 gene product, tuberin, functions as a Rab5 GTPase activating protein (GAP) in modulating endocytosis. J Biol Chem 272: 6097-6100

Yamamoto T, Pipo JR, Feng J-H, Takeda H, Nanba E, Ninomiya H, Ohno K (2002). Novel TSC1 and TSC2 mutations in Japanese patients with tuberous sclerosis complex. Brain Dev 24: 227-230

Yamashita Y, Ono J, Okada S, Wataya-Kaneda M, Yoshikawa K, Nishizawa M, Hirayama Y, Kobayashi E, Seyama K, Hino O (2000). Analysis of all exons of TSC1 and TSC2 genes for germline mutations in Japanese patients with tuberous sclerosis: report of 10 mutations. Am J Med Genet 90: 123-126

Zhang H, Nanba E, Yamamoto T, Ninomiya H, Ohno K, Mizuguchi M, Takeshita K (1999). Mutational analysis of TSC1 and TSC2 genes in Japanese patients with tuberous sclerosis complex. J Hum Genet 44: 391-396